

# Why would we use the Sediment Isotope Tomography (SIT) model to establish a $^{210}\text{Pb}$ -based chronology in recent-sediment cores?

José-María Abril Hernández\*

Departamento de Física Aplicada I, ETSIA Universidad de Sevilla, Carretera de Utrera km 1, D.P. 41013 Seville, Spain

## A B S T R A C T

After half a century, the use of unsupported  $^{210}\text{Pb}$  ( $^{210}\text{Pb}_{\text{exc}}$ ) is still far off from being a well established dating tool for recent sediments with widespread applicability. Recent results from the statistical analysis of time series of fluxes, mass sediment accumulation rates (SAR), and initial activities, derived from varved sediments, place serious constraints to the assumption of constant fluxes, which is widely used in dating models. The Sediment Isotope Tomography (SIT) model, under the assumption of non post-depositional redistribution, is used for dating recent sediments in scenarios in that fluxes and SAR are uncorrelated and both vary with time. By using a simple graphical analysis, this paper shows that under the above assumptions, any given  $^{210}\text{Pb}_{\text{exc}}$  profile, even with the restriction of a discrete set of reference points, is compatible with an infinite number of chronological lines, and thus generating an infinite number of mathematically exact solutions for histories of initial activity concentrations, SAR and fluxes onto the SWI, with these two last ranging from zero up to infinity. Particularly, SIT results, without additional assumptions, cannot contain any statistically significant difference with respect to the exact solutions consisting in intervals of constant SAR or constant fluxes (both being consistent with the reference points). Therefore, there is not any benefit in its use as a dating tool without the explicit introduction of additional restrictive assumptions about fluxes, SAR and/or their interrelationship.

### Keywords:

SIT model  
 $^{210}\text{Pb}$  dating  
Recent sediments  
Chronological line  
Sediment dating

## 1. Introduction

Accurate methods for establishing chronologies for recent-sediment cores are necessary to provide reliable estimates of sediment accumulation rate (SAR) and deposition processes, which are the key for reconstructing past environmental conditions. This is possible from true varves, which occur rarely in most sedimentary sequences with the exception of lakes in glacierized basins (Ojala et al., 2012). Other non-radioactive dating methods (e.g. fossil markers, pollen, pollution markers) can provide important stratigraphic time-markers. However, radiometric dating is the only technique of general applicability that claims to provide an absolute age determination (Carroll and Lerche, 2003).

Goldberg (1963) first proposed the use of unsupported  $^{210}\text{Pb}$  ( $^{210}\text{Pb}_{\text{exc}}$  hereafter) for dating glacier ice. The method was then applied to lacustrine sediments by Krishnaswamy et al. (1971), and

Abbreviations: SIT, Sediment Isotope Tomography; SWI, sediment–water interface; SAR, sediment accumulation rate.

\* Tel.: +34 954486473; fax: +34 954486436.

E-mail address: [jmabril@us.es](mailto:jmabril@us.es).

to marine sediments by Koide et al. (1972). After half a century, its use has been widely spread, with new models of increased complexity and applying to a large diversity of scenarios, including lakes, estuaries, reservoirs, riverine floodplains, wetlands, salt-marshes, coastal areas and marine environments (see the review papers by Appleby, 2008; Mabit et al., 2014). Nevertheless, the method is still far off from being a well-established dating technique applicable to all situations. Thus, Smith (2001) pointed out the constraints in the use of stand-alone  $^{210}\text{Pb}$ -based models and claimed for the need of validation of the so derived chronologies against independent stratigraphic time marks. These latest can be provided by some bomb-fallout radionuclides (mainly  $^{137}\text{Cs}$ ,  $^{241}\text{Am}$  and  $^{239+240}\text{Pu}$ ) through the identification of their characteristic peak values within their respective depth profiles in the sediment core. Consequently, in recent years the combined use of  $^{210}\text{Pb}$  and these bomb-fallout radionuclides has been widely popularized in the radiometric dating of recent sediments, accounting for one of the most interesting applications of the environmental radioactivity. As result, our level of understanding of the potentials and limitations of these dating tools has been also considerably improved.

Different models (each one being a set of assumptions about the functioning of the studied sedimentary system) arise as particular

solutions of a unique physical problem of advective-diffusive transport of particle-associated radionuclides in sediments, treated as continuous media that have undergone accretion and compaction (Abril, 2003a, 2011). In some cases the behavior of the dissolved fraction of radionuclides requires handling separate equations for the dissolved and the particle-bound phases (Robbins and Jasinski, 1995; Abril and Gharbi, 2012). Almost all models assume ideal deposition as a boundary condition at the sediment water interface (SWI), i.e. new radioactive inputs will be deposited above the previously existing material. Abril and Gharbi (2012) have shown how this assumption may be unrealistic in sediment cores with very high porosities.

For the most popular and simple models, their formulation also can be established in a more straightforward way from their involved basic assumptions (see the review by Sánchez-Cabeza and Ruiz-Fernández, 2012). Thus, continuous, constant flux of  $^{210}\text{Pb}_{\text{exc}}$  to the SWI, along with the absence of post-depositional redistribution, constitute the basis for the constant rate of supply (CRS) model, which contains, as a particular case, the constant flux with constant SAR (CFCS) model. The more restrictive assumption of constant fluxes and steady-state profiles is common in most  $^{210}\text{Pb}$  models because it enables analytical solutions (Robbins, 1978; Abril, 2003a). The constant initial concentration (CIC) model (Goldberg, 1963) assumes that the fluxes of matter through the SWI always carry the same activity concentration. Recently, Abril and Brunskill (2014) revisited these assumptions through the statistical analysis of a database of laminated sediments. The reconstructed historical records of  $^{210}\text{Pb}_{\text{exc}}$  flux onto the SWI, SAR, and initial  $^{210}\text{Pb}_{\text{exc}}$  activity, showed large temporal fluctuations. They found that there was no statistically significant correlation between initial activity and SAR, violating an assumption of most  $^{210}\text{Pb}$ -based radiometric dating models. Nevertheless,  $^{210}\text{Pb}_{\text{exc}}$  fluxes were linearly related with SAR (at 99% confidence level, and explaining 2/3 of the observed variability). These results can be explained through a two-component mass flow model with intrinsic scatter (Abril and Brunskill, 2014).

The Sediment Isotope Tomography (SIT) model (Carroll and Lerche, 2003) claims its ability for dating sediment cores under varying conditions for both SAR and  $^{210}\text{Pb}_{\text{exc}}$  flux. After Abril and Brunskill (2014), there are serious constraints in the applicability of models that assume constant flux, and then the SIT model could be seen as the definitive modelling tool for routinely use (restricted to situations with ideal deposition and non post-depositional mixing). Its use has remained perhaps limited by its mathematical complexity and the challenges of its programming, what could be surpassed by a broad availability of suitable software. This paper revisits the physical basis behind the mathematical formulation of the SIT model, and explores its limitations.

## 2. Material and methods

Instead of complex mathematics, a quite intuitive graphical method for establishing  $^{210}\text{Pb}_{\text{exc}}$  chronologies will be enough for present purposes.

The following assumptions stand behind the application of the basic SIT model: i)  $^{210}\text{Pb}_{\text{exc}}$  behaves as a particle-associated tracer and new inputs are ideally deposited at the SWI over the previously existing material; ii) there is not any post-depositional redistribution (what implies that compaction does not involve true mass-transport processes, such as transport of colloids and small-grain size particles through the connected water pores); iii) continuity of the sequence (i.e., there is not any missing layer by erosion).

For conceptual simplicity it will be considered that the sediment core can be sliced with an extremely high resolution, and that  $^{210}\text{Pb}_{\text{exc}}$  can be estimated as accurately as desired. The actual depth is not an

appropriate magnitude due to compaction during the sediment accretion and to the shortening during the coring operation and later handling. The mass depth magnitude must be used instead. A  $^{210}\text{Pb}_{\text{exc}}$  versus mass depth profile can be plotted as a continuous line which extends till  $m_{\text{max}}$ , corresponding to the end of the sampled core or to the deepest measured slice. Although the profile usually is an overall decreasing function that can contain some intermediate relative maxima, it is not necessary to include any additional hypothesis at this stage. An example is shown in Fig. 1 (a synthetic profile generated by the analytical function  $A(m) = 500(1 + 0.2 \sin(\pi m/2)) \exp(-\lambda m/0.07)$ ) with  $m_{\text{max}} = 6 \text{ g cm}^{-2}$ ). The goal is to find out a chronology from this data set.

A chronology can be plotted as a continuous line (by the assumption of the continuity of the sequence) in the age ( $T$ ) versus mass depth ( $m$ ) plane. The chronological line must be confined within a rectangle defined by  $m_{\text{max}}$  and the practical upper limit associated to the radioactive measurements (usually  $^{210}\text{Pb}$  cannot be measured in sediment slices older than 100–150 years). Any continuous and increasing ( $dT/dm > 0$ ) function confined within such limits is a mathematical solution for our problem (i.e. any continuous line that one can plot with a pencil without moving it down). Some examples appear in Fig. 2 (which also includes other details that will be presented further below). The local derivative at any value of  $m$  (related to the local slope of the chronological line) is related with the mass sediment accumulation rate (SAR),  $w$ , at the former position of the SWI (when took place the formation of the layer now being at a mass depth  $m$ ):

$$w = \frac{dm}{dT} ; \quad \frac{dT}{dm} = \frac{1}{w} \quad (1)$$

Thus, an almost horizontal segment in the chronological line corresponds to an episode of extremely high SAR, and a vertical segment corresponds to a period of time without sedimentation. Any straight line within the admissible boundaries is a chronological line that represents a sedimentary scenario under constant SAR.

For any given chronological line  $T(m)$ , one can obtain for each value of  $m$  the corresponding value of  $w(T)$  by using Eq. (1).  $A(m)$  is the value of  $^{210}\text{Pb}_{\text{exc}}$  activity concentration in the sediment slice at mass depth  $m$ . From the involved assumptions it is possible to estimate the  $^{210}\text{Pb}_{\text{exc}}$  activity at the former SWI,  $A_{\text{SWI}}(T)$ :

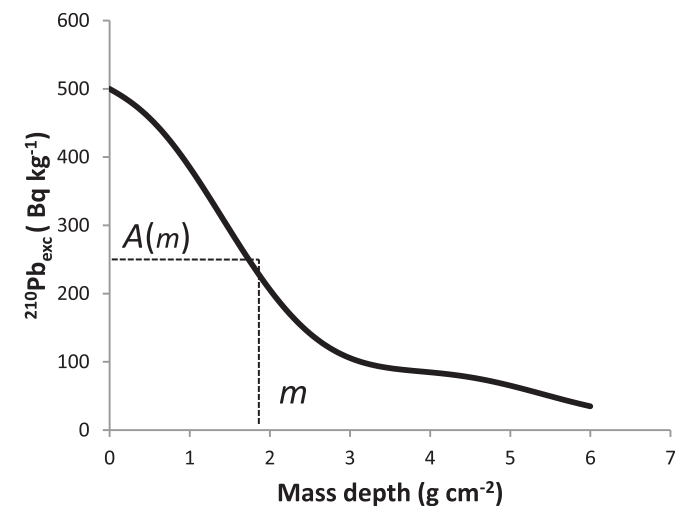
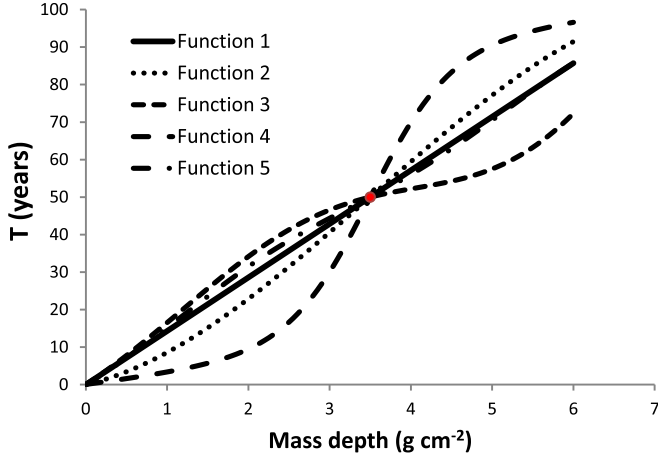


Fig. 1. Example of  $^{210}\text{Pb}_{\text{exc}}$  activity ( $A$ ) versus mass depth ( $m$ ) profile. Synthetic profile generated by the analytical function  $A(m) = 500(1 + 0.2 \sin(\pi m/2)) \exp(-\lambda m/0.07)$  with  $m_{\text{max}} = 6 \text{ g cm}^{-2}$ .



**Fig. 2.** Examples of chronological lines satisfying continuity, positive derivative and passing through the reference point (red dot). See text for the analytical expressions. (For interpretation of the references to colour in this figure legend, the reader is referred to the web version of this article.)

$$A(m) = A_{SWI}(T)\exp(-\lambda T); \quad (2)$$

where  $\lambda$  is the radioactive decay constant for  $^{210}\text{Pb}$ . Finally, it is possible to estimate the  $^{210}\text{Pb}_{\text{exc}}$  flux at the former SWI:  $F(T) = A_{SWI}(T)w(T)$ . It is worth noting that  $F$  is the flux at the SWI, conceptually different from the atmospheric deposition.

Only after handling additional information to that already contained in the  $^{210}\text{Pb}_{\text{exc}}$  profile, it is possible to discard some mathematically exact solutions as being physically unlikely (e.g. an step-like chronological line may represent a single sediment depositional episode covering a certain mass thickness interval, but in proven cases, when this happen,  $^{210}\text{Pb}_{\text{exc}}$  activities within do not use to show a continuous trend of decreasing – see examples in Sugai et al., 1994; Aalto and Nittrouer, 2012). In all the cases, both SAR and  $F$  values can range from approaching zero up to infinity. The introduction of additional assumptions such as the constancy of fluxes and/of SAR allows to find out a chronological line as unique and exact mathematical solution. Of course, the reliability of such assumptions needs an independent validation.

In the most general case, neither fluxes, nor SAR remain constant over time. The SIT model claims its ability to find out a constrained set of mathematical solutions for  $w(T)$  and  $F(T)$  under such conditions. As many combinations of model coefficients will fit a given data profile to within the same level of uncertainty, to reduce the number of model-determined answers, an independent time marker, such as  $^{137}\text{Cs}$ , can be input to the model (Carroll and Lerche, 2003). This is, we must know the age of one or more sediment slices (each one is a point in the age versus mass depth plane). To illustrate this, Fig. 2 includes one reference point at mass depth  $3.5 \text{ g cm}^{-2}$ , with and age of 50 years. The same Fig. 2 includes five examples of chronological lines satisfying continuity, positive derivative, and passing through the reference point. They serve only as illustration, and these are their analytical expressions (F1 to F5 correspond to functions 1 to 5 in Fig. 2):

$$F1(m) = m/0.07$$

$$F2(m) = -0.381m^3 + 4.000m^2 + 4.955m$$

$$F3(m) = m/0.07 + (2.857m)\sin(\pi m/3.5)$$

$$F4(m) = \frac{80}{1 + \exp[2(3.5 - m)]} + 2.857m$$

$$F5(m) \equiv \text{CRS model}$$

F5 corresponds to the CRS model forced by the reference point method. The corresponding histories of SAR (from Eq. (1)), initial activity (from Eq. (2)), and fluxes onto the SWI are depicted in Fig. 3. These five quite different histories are all they exact mathematical solutions of the stated problem, and, at a first glance, they are all physically feasible.

Fig. 4 shows how two reference points constrain the possible chronological lines. The chronological lines must be now confined within the sub-rectangles defined by the reference points (the shaded ones in Fig. 4), but the number of mathematically exact solutions still remains infinite. The rectangle's borders correspond

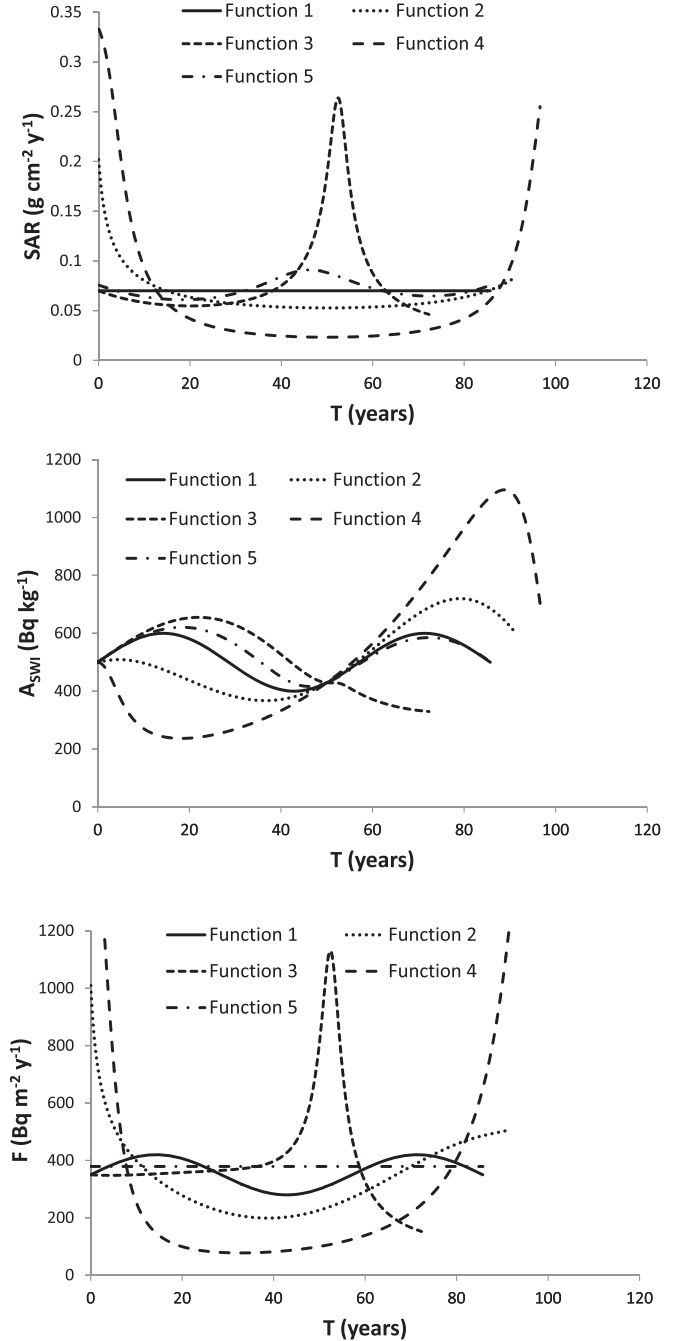


**Fig. 3.** Histories of SAR (Eq. (1)), initial activity, and fluxes onto the SWI (Eq. (2)), generated from the synthetic  $^{210}\text{Pb}_{\text{exc}}$  profile (Fig. 1) and the five chronological lines depicted in Fig. 2.

to extreme cases of a single depositional event preceded or followed by a time lapse without sedimentation. The straight line connecting the reference points is another exact solution that corresponds to periods of constant SAR. For a single reference point it is mathematically possible (by adapting the value of the total inventory) finding out a solution for the constant rate of supply (CRS) model, and for two or more reference points, a solution with different periods of constant fluxes.

### 3. Results and discussion

#### 3.1. Mathematical basis for the SIT model in perspective

The chronological function, multiplied by the radioactive decay constant, can be split into two functions:  $\lambda T(m) = Bm + f(m)$ , where  $B$  is a constant and  $f(m)$  is continuous and verify  $f(0) = 0$ . Thus, it is possible to write:

$$\lambda T(m) = Bm + \sum_{n=1}^{\infty} a_n \sin\left(\frac{n\pi m}{m_{\max}}\right),$$

$$\text{with } a_n = \frac{2}{m_{\max}} \int_0^{m_{\max}} f(m) \sin\left(\frac{n\pi m}{m_{\max}}\right) dm. \quad (3)$$

It is worth noting that there is not any physical law behind this particular choice (sine, cosine, or combined series are equally possible), and that the Fourier series plus the term  $Bm$  converge to  $\lambda T(m)$ , and consequently it satisfies the requirements of continuity and positive derivative within the interval  $[0, m_{\max}]$ .

For convenience,  $A_{SWI}(m)$  can be rewritten as  $A_{SWI}(m) = A_{SWI}(0) \exp(g(m))$ , where  $g(m)$  is continuous and satisfies  $g(0) = 0$ . Finally, and from Eq. (2), it is possible to write:

$$A(m) = A_{SWI}(0) \exp\left\{ - \left[ Bm + \sum_{n=1}^{\infty} a_n \sin\left(\frac{n\pi m}{m_{\max}}\right) \right] + \left[ \frac{b_0}{2} + \sum_{n=1}^{\infty} b_n \cos\left(\frac{n\pi m}{m_{\max}}\right) \right] \right\} \quad (4)$$

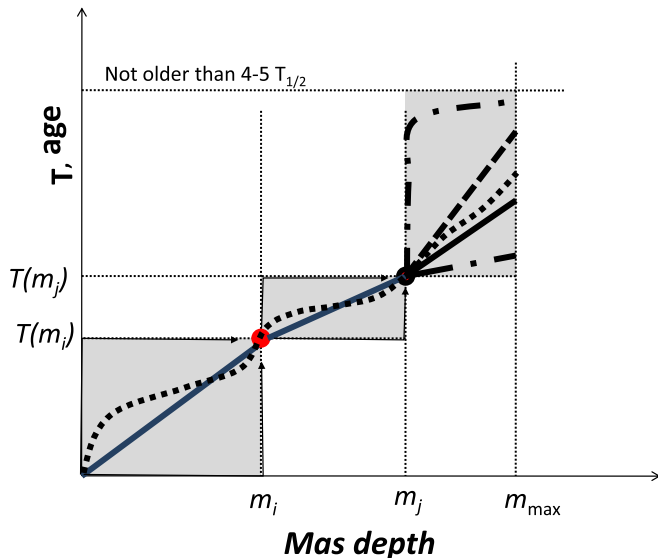


Fig. 4. Diagram showing examples of chronological lines constrained by two reference points.

The coefficients  $a_n$  and  $b_n$  are found, respectively, from  $f(m)$  and  $g(m)$  functions. The SIT model uses Eq. (4) (or an alternative equivalent formulation) to extract the coefficients  $a_n$  and  $b_n$  from  $A(m)$ , instead from  $f(m)$  and  $g(m)$ . The so obtained coefficients do not represent the physical problem of a chronological line. This is a conceptual flaw in the SIT model, only partly compensated by additionally imposing the condition of positive derivative for the so constructed function  $T(m)$ .

More precisely, by operating in Eq. (4), one can construct the function  $h(m) = \ln[A(m)/A_{SWI}(0)] + Bm$ , which is continuous, defined in  $[0, m_{\max}]$ , and it can be expanded into a combined sine and cosine Fourier series. This last formally requires defining a branch of the function  $h(m)$  in the interval  $[-m_{\max}, 0)$  and ensuring its periodicity. Obviously, there are an infinite number of possibilities for such an extension ( $h(m) = 0$  is only one of them), and in all the cases the Fourier series containing sine and cosine terms will converge to the known branch of  $h(m)$  in the interval  $[0, m_{\max}]$ . Thus,  $a_n$  and  $b_n$  coefficients are not univocally defined, although they may be forced by reference points.

To illustrate this point, Fig. 5a shows the analytical function  $h(m)$ ,  $h_0$  in the plot, corresponding to the synthetic profile of Fig. 1 (by using  $B = \lambda/0.07$ ), along with 5 Fourier series with sine and cosine terms ( $N = 100$ ) resulting from the following extensions of  $h(m)$  for the  $[-m_{\max}, 0)$  interval:  $h(m) = 0.055m^2 + 0.333m$  (curve h1);  $h(m) = -0.055m^2 - 0.333m$  (curve h2);  $h(m) = -0.15$  (curve h3);  $h(m) = -h(-m)$  (curve h4);  $h(m) = -h(-m) - 0.3$  (curve h5). In all the cases, the Fourier series converge to  $h(m)$  – and thus, to  $A(m)$ , in the positive interval (in Fig. 5a all the lines are superposed; the noise at the two boundaries is due to the known Gibbs phenomenon). Although they converge to the same function, the involved coefficients are different, leading then to different chronological lines, as illustrated in Fig. 5b. Two of them (h3 and h5) match the reference point but with different SAR histories. The number of possibilities for selecting an extension of  $h(m)$  able to generate suitable chronological lines fitting the reference points is infinite. In the SIT model formulation (Carroll and Lerche, 2003), the coefficients  $a_n$  and  $b_n$  are obtained by integration in the interval  $[0, m_{\max}]$ , what implicitly assumes  $h(m) = 0$  in the symmetric negative interval, and thus introducing a spurious bias in the number of possible mathematically exact solutions. There is not a straightforward translation of this restriction into physical terms.

In any practical problem,  $A(m)$  is known not as a continuous function but as a step-function (over the mass thickness interval of each sediment slice), with the involved measurement uncertainties that also affect to the reference points. On the other hand, it is not possible to handle an infinity number of terms in the Fourier series; thus, numerical approximations are mandatory. Due to the involved uncertainties,  $A(m)$  and  $T(m)$  functions that only approximately match the measured profile and the reference points are also admissible, so the criteria of minimizing a chi-square function can be applicable. In the SIT model, results for chronology,  $T(m)$ , and SAR history,  $w(T)$ , are provided with their associated uncertainties. The meaning of such error estimate has to be put into the scope of the reasons for excluding other mathematically exact solutions.

#### 3.2. Application to a real case study

Fig. 6 shows the estimated  $^{210}\text{Pb}_{\text{exc}}$  versus mass depth profile reported by Tylmann et al. (2013) for the varved sediment core LAZ 07/2 from Lake Łazduny (northern Poland, sampled in 2007 at  $53^\circ 51.40'N$ ,  $21^\circ 57.30'E$ ; 20–20.5 m depth). This core, included in the compilation by Abril and Brunskill (2014), will serve as a real case study. Vertical bars correspond to the associated uncertainties, while the horizontal ones define de mass depth interval of each sediment slice (it is worth noting that these  $^{210}\text{Pb}_{\text{exc}}$  values are

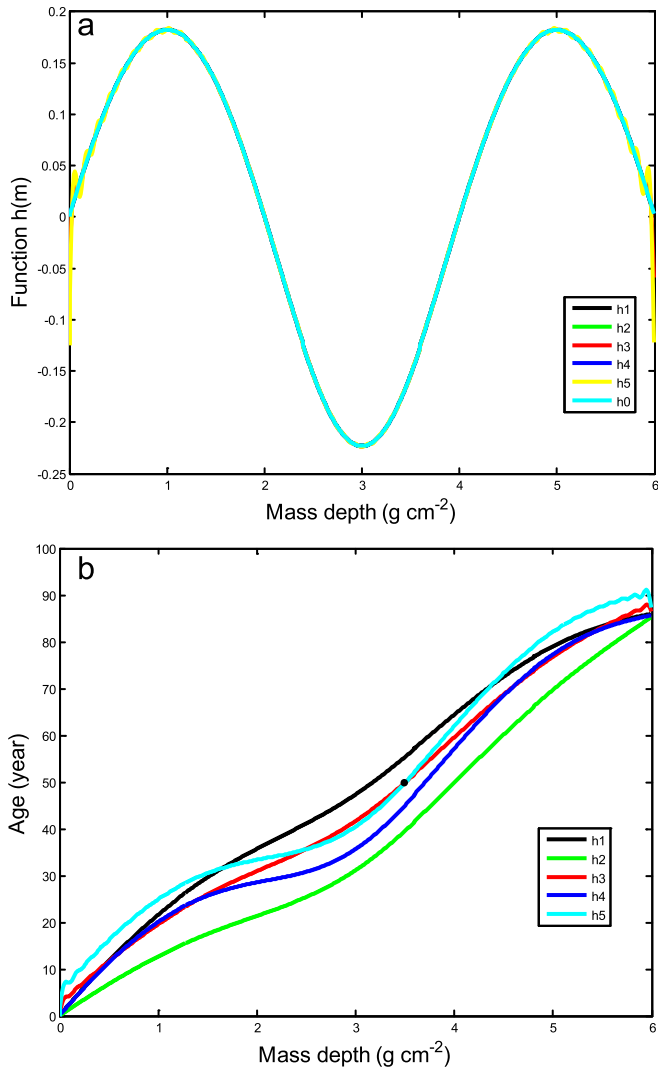


**Fig. 5.** a) Analytical function  $h(m)$ ,  $h_0$  in the plot, corresponding to the synthetic profile of Fig. 1 (by using  $B = \lambda/0.07$ ), along with 5 Fourier series with sine and cosine terms ( $N = 100$ ) resulting from the following extensions of  $h(m)$  for the  $[-m_{\max}, 0)$  interval:  $h(m) = 0.055m^2 + 0.333m$  (curve  $h_1$ );  $h(m) = -0.055m^2 - 0.333m$  (curve  $h_2$ );  $h(m) = -0.15$  (curve  $h_3$ );  $h(m) = -h(-m)$  (curve  $h_4$ );  $h(m) = -h(-m) - 0.3$  (curve  $h_5$ ). b) The corresponding chronological lines and the reference point (black dot).

operationally averaged values over the mass thickness interval of the sediment slice). Tylmann et al. (2013) measured the  $^{137}\text{Cs}$  profile, which showed two distinct peaks at the 4–5 cm and 7–8 cm intervals, attributable, respectively, to the 1986 Chernobyl accident and to the 1963 bomb-fallout maximum. These peaks will provide two reference points for the chronology that is intended to be derived from the  $^{210}\text{Pb}_{\text{exc}}$  profile.

Fig. 7a shows a set of five arbitrarily selected chronological lines (denoted as F1 to F5) passing through the reference points. The corresponding averaged SAR values over the time intervals associated to each sediment slice are depicted in Fig. 7b. For the sake of clarity the propagated uncertainties are not shown, and the mean value of SAR is plotted at the central point of each slice interval (continuous lines are only for guiding-eyes). The continuous step line in Fig. 6 corresponds to an analytical solution, plotting the averaged values over the time interval associated to each sediment slice. It can be compared against the empirical data through the usual  $\chi^2$  function that involves

the associated uncertainties, leading in this case to a value of zero. Thus, this solution cannot be excluded from the SIT model answers by any criteria of minimizing  $\chi^2$ . It serves to reconstruct the historical fluxes onto the SWI from the chronological line as done in the methods section. Results are shown in Fig. 7c.

The chronological line F1 has two transects: the first one is a linear interpolation between the origin and the first reference point, and the second one continues passing through the second reference point. Lines F2 and F3 are variations from F1, dividing each transect into two parts with external points. Line F4 progresses with random variations in the slope, while line F5 is a parabolic fit to the reference points forced through the origin. In all the cases fluxes and SAR vary with time, and they all are mathematically exact solutions for the stated problem.

Fig. 7a includes the SIT chronology derived from the empirical  $^{210}\text{Pb}_{\text{exc}}$  profile and constrained by the two reference points (from Tylmann et al., 2013). This chronological line, when plotted against actual depths is a straight line (slope  $5.563\ \text{y/cm}$ ,  $R^2 = 1.000$ ). The asymmetric error bars are also plotted in Fig. 7a, and it can be seen how some of the exact solutions are excluded from the confidence intervals.

The updated varve chronology for this sediment core appears in Tylmann et al. (2014), and it is shown in Fig. 7a along with the associated error bars. The averaged values for SAR for each slice interval and the estimated fluxes are also depicted in Fig. 7b and c.

A varve chronology is not available in a generic radiometric dating problem. Thus, the main question here is not the model validation. This real case example serves to illustrate that any given empirical  $^{210}\text{Pb}_{\text{exc}}$  profile, even with the additional support of several reference points, does not contain enough information to derive a chronological line as unique solution when fluxes and SAR are allowed to be independent and varying with time. And the matter is not to provide the chronological line with a proper associated uncertainty; the question is that there are always an infinity number of mathematically exact solutions with many different SAR and flux histories. Particularly, the SIT model operating only under the above assumptions cannot provide such a constrained solution.

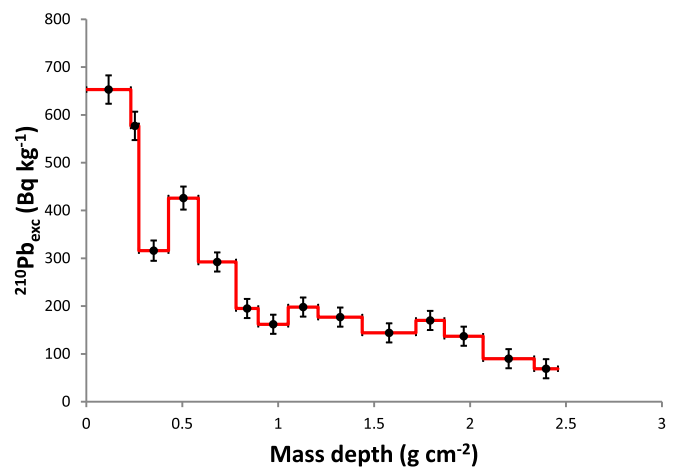


**Fig. 6.**  $^{210}\text{Pb}_{\text{exc}}$  versus mass depth profile reported by Tylmann et al. (2013) for the varved sediment core LAZ 07/2 from Lake Łazduny (northern Poland). Vertical bars correspond to the associated uncertainties, while the horizontal ones define the mass depth interval of each sediment slice. The continuous step-line represents the averaged values over each slice for the analytical solution that supports the estimations of SAR and fluxes shown in Fig. 7.

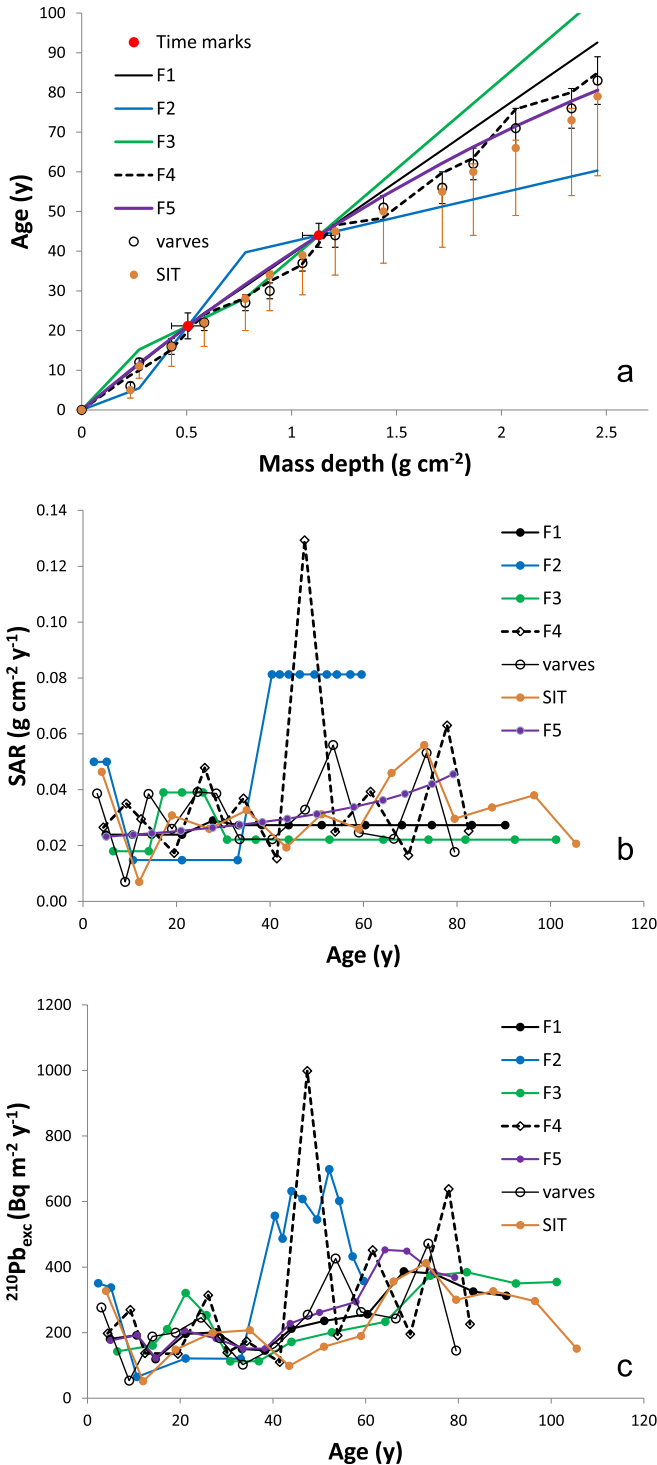


**Fig. 7.** Panel a) <sup>137</sup>Cs time marks, varve chronology and SIT ages (constrained by the <sup>137</sup>Cs time marks) for the core of Fig. 6 (data from Tylmann et al., 2014); and examples of chronological lines satisfying continuity, positive derivative and passing through the reference points (denoted as F1 to F5). Panels b and c) Histories of SAR and fluxes onto the SWI from the <sup>210</sup>Pb<sub>exc</sub> profile (Fig. 6) and the above chronological lines. Values are plotted as points at the centre of each slice interval (continuous lines are only for guiding-eyes). For the sake of clarity the propagated uncertainties have not been depicted.

A second question is that the SIT model, without explicitly imposing any restriction to the possibilities of variation of fluxes and SAR, excludes mathematically exact solutions (with  $\chi^2 = 0$ ; and thus, not being justified by criteria of minimizing errors). There is not any known criteria for thinking that the exact solutions

excluded by the SIT model are providing a wrong or a worst description of the studied sedimentary system.

The SIT model can be used as a dating tool, but accepting that the mathematical construction and the programming criteria will provide only a subset of the possible solutions involving varying SAR and fluxes. To elucidate whether this subset is the best bet, a better understanding of the translation of the SIT code into physical criteria would be required. This is also necessary to understand the meaning of the associated uncertainties in the so obtained chronology.

In this particular example, for which a varve chronology is available with known uncertainties, one can check that the SIT model has a good performance, although it ascribes high probability density in the region of low dates. The same is true for chronological lines F4 and F5 (and F1, except in the oldest layers), despite that at some points the confidence intervals are discrepant with SIT results. Concluding from this particular exercise the suitability of the SIT model performance has the same strength that the equivalent conclusion for the more straightforward quadratic fit (F5).

Finally, it is worth noting that an overall acceptable chronological line does not guarantee a confident and high resolution SAR history. SAR values are defined by the local derivative, and positive and negative deviations can be cancelled out, in average, along the chronological line, in such a way that this last does not deviate too much from the true varve chronology, but it leads to somehow spurious results for SAR. Only average SAR values estimated over relatively large time intervals in the chronological line have some physical meaning. The same is true for fluxes, since they are estimated from SAR and initial activities.

### 3.3. Constraints for <sup>210</sup>Pb-based dating models with variable and uncorrelated SAR and fluxes

Despite the involved mathematical and numerical complexity, if the <sup>210</sup>Pb-based model does not use other physical assumptions that those presented in Section 2, its results must be compatible with the known properties of the infinite number of mathematically exact solutions allowed by the graphical method. Particularly,

- i) A constant SAR (or a discrete set of episodes of constant SAR connecting every two consecutive reference points) is a mathematically exact solution, and it has to be contained within the range of solutions of the model.
- ii) A constant rate of supply for the cases of a single reference point (or a discrete series of periods of time with constant fluxes, being consistent with the reference points) is a mathematically exact solution, and it has to be contained within the range of solutions of the model.
- iii) The associated uncertainties in model results for chronologies and F(T) histories cannot contain statistically significant differences from the situations of constant SAR and constant fluxes described in i) and ii).
- iv) Model solutions cannot exclude any mathematically exact solution for the stated physical problem, and thus, they must contain SAR and fluxes ranging from zero up to infinity.
- v) The SIT model nominally operates under the above assumptions, but the used code provides a constrained subset of solutions for chronology (not necessarily better than those being excluded). The breach of the previous statements has to be attributable to mathematical artefacts or to programming criteria, as discussed in the previous section, which act as hidden assumptions. A better understanding of the translation of the SIT code into physical criteria would be

then required to properly understand its applicability and the true meaning of its results.

Restrictive assumptions about fluxes, SAR and/or their interrelationship are needed to provide a constrained solution from the  $^{210}\text{Pb}_{\text{exc}}$  data. These may be the assumptions of constant flux, constant SAR or constant initial activity, in those sedimentary scenarios where they would be properly applicable (either for the whole range of the chronology or for few sub-domains). After the recent work by Abril and Brunskill (2014) these 'classical' restrictive assumptions seem do not hold in most of the cases; instead, a statistical correlation between fluxes and SAR can be a quite general rule. Such a statistical correlation can be used to develop a new dating tool. Finally, it is worth mentioning the limitations in the mere identification of peaks in the  $^{137}\text{Cs}$  depth profiles as being suitable time markers (Abril, 2003b, 2004), being more advisable the understanding (through the use of appropriate models) of the whole profiles.

#### 4. Conclusions

Under the assumptions of continuity of the sequence, ideal deposition of  $^{210}\text{Pb}_{\text{exc}}$  fluxes and non post-depositional redistribution, any  $^{210}\text{Pb}_{\text{exc}}$  activity versus mass depth profile, even with the restriction of a discrete set of reference points, is compatible with an infinite number of chronological lines, and thus generating an infinite number of mathematically exact solutions for histories of initial activity, SAR and flux onto the SWI. Such histories may contain values of SAR and flux ranging from zero up to infinity.

Particularly, the SIT model, operating only under the above assumptions, cannot provide SAR histories with statistically significant differences with respect to the intervals of constant SAR defined by every two consecutive reference points (including  $T = 0$  for  $m = 0$ ). SIT-histories for flux cannot show statistically significant differences with respect to the intervals of constant flux being consistent with the partial inventories among the reference points. Then there is not any benefit in its use as a dating tool without the explicit introduction of additional restrictive assumptions about flux, SAR and/or their interrelationship.

#### Acknowledgements

This work was funded partially by the FIS2012-31853 Project.

#### References

- Aalto, R., Nittrouer, Ch A., 2012.  $^{210}\text{Pb}$  geochronology of flood events in large tropical river systems. *Philos. Trans. R. Soc. A* 370, 2040–2074.
- Abril, J.M., 2003a. A new theoretical treatment of compaction and the advective-diffusive processes in sediments. A reviewed basis for radiometric dating models. *J. Paleolimnol.* 30, 363–370.
- Abril, J.M., 2003b. Difficulties in interpreting fast mixing in the radiometric dating of sediments using  $^{210}\text{Pb}$  and  $^{137}\text{Cs}$ . *J. Paleolimnol.* 30, 407–414.
- Abril, J.M., 2004. Constraints on the use of Cs-137 as a time-marker to support CRS and SIT chronologies. *Environ. Pollut.* 129, 31–37.
- Abril, J.M., 2011. Could bulk density profiles provide information on recent sedimentation rates? *J. Paleolimnol.* 46, 173–186.
- Abril, J.M., Gharbi, F., 2012. Radiometric dating of recent sediments: beyond the boundary conditions. *J. Paleolimnol.* 48, 449–460.
- Abril, J.M., Brunskill, G.J., 2014. Evidence that excess  $^{210}\text{Pb}$  flux varies with sediment accumulation rate and implications for dating recent sediments. *J. Paleolimnol.* 52, 121–137.
- Appleby, P.G., 2008. Three decades of dating recent sediments by fallout radionuclides: a review. *Holocene* 18, 83–93.
- Carroll, J., Lerche, I., 2003. *Sedimentary Processes: Quantification Using Radionuclides*. Elsevier, Oxford.
- Goldberg, E.D., 1963. Geochronology with Pb-210. In: *Proceedings of a Symposium of Radioactive Dating*. International Atomic Energy Agency, Vienna, pp. 121–131.
- Koide, M., Soutar, A., Goldberg, E.D., 1972. Marine geochronology with  $^{210}\text{Pb}$ . *Earth Planet. Sci. Lett.* 14, 442–446.
- Krishnaswamy, S., Lal, D., Martin, J.M., Meybek, M., 1971. Geochronology of lake sediments. *Earth Planet. Sci. Lett.* 11, 407–414.
- Mabit, L., Benmansour, M., Abril, J.M., Walling, D.E., Meusburger, K., Iurian, A.R., Bernard, C., Tarján, S., Owens, P.N., Blake, W.H., Alewell, C., 2014. Fallout  $^{210}\text{Pb}$  as a soil and sediment tracer in catchment sediment budget investigations: A review. *Earth Sci. Rev.* 138, 335–351.
- Ojala, A.E.K., Francus, P., Zolitschka, B., Besonen, M., Lamoureux, S.F., 2012. Characteristics of sedimentary varve chronologies— a review. *Quat. Sci. Rev.* 43, 45–60.
- Robbins, J.A., 1978. Geochemical and geophysical applications of radioactive lead isotopes. In: Nriago, J.P. (Ed.), *Biochemistry of Lead in the Environment*. Elsevier, Amsterdam, pp. 285–393.
- Robbins, J.A., Jasinski, A.W., 1995. Chernobyl fallout radionuclides in Lake Sniardwy, Poland. *J. Environ. Radioact.* 26, 157–184.
- Sánchez-Cabeza, J.A., Ruiz-Fernández, A.C., 2012.  $^{210}\text{Pb}$  sediment radiochronology: an integrated formulation and classification of dating models. *Geochim. Cosmochim. Acta* 82, 183–200.
- Smith, J.N., 2001. Why should we believe  $^{210}\text{Pb}$  sediment geochronologies? *J. Environ. Radioact.* 55, 121–123.
- Sugai, S.F., Alperin, M.J., Reeburgh, W.S., 1994. Episodic deposition and  $^{137}\text{Cs}$  immobility in Skan Bay sediments: a ten-year  $^{210}\text{Pb}$  and  $^{137}\text{Cs}$  time series. *Mar. Geol.* 116, 351–372.
- Tylmann, W., Enters, D., Kinder, M., Moska, P., Ohlendorf, Ch, Poreba, G., Zolitschka, B., 2013. Multiple dating of varved sediments from Lake Łazduny, northern Poland: toward an improved chronology for the last 150 years. *Quat. Geochronol.* 15, 98–107.
- Tylmann, W., Fischer, H.W., Enters, D., Kinder, M., Moska, P., Ohlendorf, Ch, Poreba, G., Zolitschka, B., 2014. Reply to the comment by F. Gharbi on "Multiple dating of varved sediments from Lake Łazduny, northern Poland: toward an improved chronology for the last 150 years". *Quat. Geochronol.* 20, 11–113.